Journal of Applied Polymer Science

Synthesis and Characterization of Chitosan-*graft*-Poly(acrylic acid)/Nontronite Hydrogel Composites Based on a Design of Experiments

Francisco H. A. Rodrigues,[1,2] Antonio G. B. Pereira,[2] André R. Fajardo,[2] Edvani C. Muniz[2]

[1]Coordenação de Química, Universidade Estadual Vale do Acaraú, Avenida da Universidade, 850, Campus da Betânia, 62040-370, Sobral, Ceará, Brazil

[2]Grupos de Materiais Poliméricos e Compósitos, Departamento de Química, Universidade Estadual de Maringá, Avenue Colombo, 5790, 87020-900, Maringá, Paraná, Brazil

Correspondence to: F. H. A. Rodrigues (E-mail: almeida_quimica@yahoo.com.br)

ABSTRACT: A 2^{4-1} fractional factorial design was used to evaluate the effect of some parameters, such as the acrylic acid (AA)/chitosan (CTS) molar ratio, crosslinker concentration, initiator concentration, and filler concentration, in the swelling capacity of superabsorbent hydrogel composites based on CTS-*graft*-poly(acrylic acid) and nontronite clay. The data from wide-angle X-ray scattering and Fourier transform infrared spectroscopy confirmed the syntheses of the hydrogel composites. Main and interaction effects were analyzed by analysis of variance, *F* tests, and *p* values. We found that the AA/CTS and crosslinker were the most influential effects in the evaluated response. The proposed statistical model presented a high coefficient of determination ($R^2 = 0.985$). In addition to the swelling kinetics, the effects of pH and salt for the both compositions (with and without filler), which presented the best water uptake, were evaluated. Both hydrogels showed responsive behavior in relation to the pH and the salt solution, presenting good potential for application as devices in the controlled release of solutes. © 2012 Wiley Periodicals, Inc. J. Appl. Polym. Sci. 128: 3480–3489, 2013

KEYWORDS: clays; composites; hydrogels; nanocomposites

revised 29 May 2012; accepted 24 July 2012; published online 28 September 2012

DOI: 10.1002/app.38386

INTRODUCTION

Superabsorbent hydrogels are loosely crosslinked polymers that can absorb and retain an outstanding volume of aqueous fluids, amounts as high as 100–1000 times their weight, even under pressure due to the presence of large amounts of hydrophilic groups.[1] Because of their characteristics, such materials have been applied in many fields, including agricultural,[1] biomedical,[2] and hygienic products.[3] Although superabsorbent hydrogels made of synthetic polymers (mainly based on acrylate and acrylamide monomers) present excellent water uptake capability and mechanical properties, the lack of degradation under environmental conditions and their possible toxicity raise great ecological and health concerns. In light of this, many researchers have focused on the introduction of natural polymers [e.g., starch,[4] chitosan (CTS),[5] and arabic gum[6]] by grafting synthetic polymers to the biopolymer backbone rendering biodegradable, biocompatible, and/or superabsorbent hydrogels.[7,8]

It is well know that many biopolymers do not present satisfactory mechanical and/or thermal properties.[9,10] However, it has been shown that the swelling capability, strength, and thermal behavior can be tuned through the addition of organic fillers (e.g., cellulose,[11,12] starch,[13] and chitin[13] nanocrystals) and inorganic fillers (e.g., magnetic nanoparticles,[14] ash,[15] and clays such as montmorillonite,[16] vermiculite,[17] and bentonite[18]) with nanometric dimensions due to the formation of nanocomposite materials.

In this study, we discovered that the swelling properties of CTS-*graft*-poly(acrylic acid) (PAA) hydrogels could be tuned through the addition of nontronite clay (NONT), an iron-rich smectite with a dioctahedral structure.[19,20] CTS, a well-known polymer, was chosen because of its interesting physical and biological properties (i.e., biocompatibility, biodegradability, low toxicity, antibacterial and hemostatic activities, and chelating potential).[21,22] CTS acted as a desirable backbone for grafting PAA to form a superabsorbent material. In addition, to the best of our knowledge, hydrogel composites containing NONT have not been reported in the literature until now.

EXPERIMENTAL

Materials

Acrylic acid (AA) and potassium persulfate ($K_2S_2O_8$) were purchased from Sigma-Aldrich, St. Louis, MO. *N, N′*-Methylene bisacrylamide (MBA) was purchased from Pharmacia Biotech (GE Healthcare, São Paulo, Brazil). CTS (85% deacetyled) was purchased from Golden-Shell Biochemical (Zhejiang, China) and

Table I. Design of the Experiments

	Two-level factors				
Sample	*A* (mol %)	*B* (wt %)	*C* (wt %)	*D* (wt %)	Water uptake (g of water/g of absorbent)
1	(−1) 5	(−1) 1	(−1) 1	(−1) none	204
2	(+1) 10	(−1) 1	(−1) 1	(+1) 10	433
3	(−1) 5	(+1) 3	(−1) 1	(+1) 10	121
4	(+1) 10	(+1) 3	(−1) 1	(−1) none	127
5	(−1) 5	(−1) 1	(+1) 3	(+1) 10	262
6	(+1) 10	(−1) 1	(+1) 3	(−1) none	381
7	(−1) 5	(+1) 3	(+1) 3	(−1) none	72
8	(+1) 10	(+1) 3	(+1) 3	(+1) 10	225
9	(0) 7.5	(0) 2	(0) 2	(−1) none	188
10	(0) 7.5	(0) 2	(0) 2	(+1) 10	281

presented an average viscometric molar mass (M_V) of 87 kDa. M_V was obtained according to methodology previously described by Fajardo et al.[23] The NONT was kindly donated by Empresa Bentonita do Nordeste situated at Paraiba state (Paraíba, Brazil). It was previously ground and sieved through a 325-mesh (44 μm) sieve. The clay had a cationic exchange capacity of 145 mequiv/100 g, and the chemical composition obtained by X-ray fluorescence was as follows: [Silicon] = 5.32 mequiv/g, [Iron] = 0.82 mequiv/g, [Aluminum] = 0.60 mequiv/g, [Sodium] = 0.48 mequiv/g, [Magnesium] = 0.12 mequiv/g, and [Calcium] = 0.08 mequiv/g.

Preparation of the CTS-*graft*-PAA/NONT Hydrogel Composites

A series of hydrogel composites based on CTS, AA, and NONT were prepared according to the following procedure: an appropriate amount of CTS was solubilized under magnetic stirring in 30 mL of acetic acid solution (1 v/v %) in a three-necked flask equipped with a reflux condenser, a funnel, and an $N_{2(g)}$ line. The CTS solution was purged for 30 min to remove the oxygen. After this, the solution was heated to 70°C, and then, potassium persulfate was introduced to generate free radicals on the CTS chains. Ten minutes later, another solution, which consisted of AA and specific amounts of MBA and NONT in 5 mL of distilled water, was added to the CTS solution. The resulting solution was heated for 3 h to complete the formation of the CTS-*graft*-PAA/NONT hydrogel composite. Therefore, the produced hydrogel, which was present in granular form, was cooled to room temperature (ca. 25°C) and then neutralized to pH 7.0 with the addition of an NaOH aqueous solution. The CTS-*graft*-PAA/NONT hydrogel was washed with large volumes of distilled water to remove residual reactants and then oven-dried at 70°C. The sizes of the particles fell within the 9–24-mesh range (0.71–2.00 mm). In addition, a blank sample, without NONT, was prepared according to procedures described previously. This sample was labeled CTS-*graft*-PAA.

Statistical Evaluation of the Parameters by a Factorial Design Approach

To verify the influence of some of the parameters on the water uptake capacity (in distilled water) of the CTS-*graft*-PAA/NONT hydrogel composite a fractional factorial design (FFD) was performed. It was applied to a 2^{4-1} FFD, in which we tested four parameters: AA/CTS molar ratio (*A;* numeric), crosslinker concentration (*B;* numeric), initiator concentration (*C;* numeric), and filler concentration (*D;* categoric). Each parameter was varied in two levels, and two center points were used. This resulted in 10 runs. The coded variables −1, 0, and +1 represent low, intermediate, and high levels (see Table I). The FFD and the evaluation of the results based on analysis of variance (ANOVA) were carried out with Design Expert (version 7.1.3) software (Minneapolis, MN).

Methods of Characterization

Fourier Transform Infrared (FTIR) Spectroscopy. All of the dried hydrogel composites and the blank sample were characterized by the FTIR technique with a transform infrared spectrophotometer (Shimadzu Scientific Instruments, model 8300, Columbia, MD) operating in the region from 4000 to 500 cm^{-1} at a resolution of 4 cm^{-1}. The dried material was blended with KBr powder and pressed into tablets before spectrum acquisition.

Wide-Angle X-ray Scattering (WAXS). The WAXS patterns were obtained in a diffractometer (DMAXB, Rigaku, Texas USA) equipped with a Cu Kα radiation source (30 kV and 20 mA) with a scattering angle (2θ) from 5 to 70° at a resolution of 0.02° and with a scanning speed of 2°/min.

Scanning Electron Microscopy (SEM). The hydrogel composite morphologies were evaluated through SEM images obtained from a scanning electron microscope (Shimadzu, model SS550 Superscan). The samples were gold-coated by a sputtering technique before the analyses.

Study of the Swelling Properties

Swelling Assays. Initially, swelling assays were used to determine the water absorption capacities of the materials (CTS-*graft*-PAA and CTS-*graft*-PAA/NONT). In this way, 15 mg of each sample tested was placed in a 30-mL filter crucible (porosity number = 0) premoistened with a dry outer wall. This set was inserted in water in such a way that the gel was completely submerged. The crucible/composite hydrogel samples sets were

Table II. ANOVA of Swelling: Effects of A, B, and D

Source	Sum of squares	DF	Mean square	*F*	*p* ($p > F$)
Model	1.164×10^5	4	29,093.59	113.84	0.0014[a]
A	32,131.12	1	32,131.12	123.52	0.0016
B	67,528.13	1	67,528.13	250.60	0.0005
D	8256.12	1	8256.12	31.74	0.0111
AB	4465.13	1	4465.13	17.17	0.0255
Residual	780.38	3	260.13		
Cor total	1.176×10^5	9			

[a]Model significant ($R^2 = 0.9933$, adjusted $R^2 = 0.9845$).
DF = Degrees of Freedom.

removed at specific time intervals, the external wall of the set was dried, and the system was weighed. For each sample, three assays were performed. The swelling capacity of the hydrogel composites was determined from eq. (1):

$$W = [m/m_0] - 1 \quad (1)$$

where W is the gained water mass [g/g of composite hydrogel (absorbent)], m is the mass of the swollen absorbent, and m_0 is the mass of the dry material.[24] It was possible to follow the kinetics of swelling in each studied medium. The size distribution of the hydrogel composites remained in the 9–24 mesh range

Effect of the Salt Solution on the Water Absorbency. The hydrogel composites were immersed in distinct aqueous salt solutions (concentration = 0.15 mol/L) and their swelling capabilities were determined according to the procedures described previously. To study the effect of the type of ions as counterions of salt, solutions of NaCl and $NaHCO_3$ were used to verify the anion effect, and solutions of NaCl, KCl, NH_4Cl, $CaCl_2$, and $AlCl_3$ were used to evaluate the cation effect, with all solutions having a fixed ionic strength ($I = 0.1$ *M*).

Evaluation of the pH Effect on the Swelling Capability of the Hydrogel Composites. The effect of the pH on swelling was also verified in buffer solutions (pH 2–12). The ionic strength was kept constant at 0.1 *M*.

RESULTS AND DISCUSSION

2^{4-1} FFD

The swelling properties of hydrogels can be tailored through changes in the experimental conditions applied to their formation. Several variables in the hydrogel formation (e.g., polymer concentration, contents of crosslinking agents and gelling initiators, and addition of filler) have been discussed extensively as intrinsic factors that affect its swelling performance.[25,26] Because the swelling is dependent on many factors, the use of a factorial design of experiments seems to be very suitable for understanding how such factors are related to each other and to the swelling capacity. In this study, a factorial design was used to evaluate the influence of some factors on the water uptake capacity of a CTS-*graft*-PAA based hydrogel. Table I presents the level of all of the factors we evaluated for each run with the respective response (the water uptake capacity).

From the FFD of experiments, it was possible to evaluate the main effect and the interaction effects by ANOVA. ANOVA is a statistical tool that allows the evaluation of different sources of variation that contribute to the observed variance for a specific factor.[27] Through ANOVA, we determined that the main effects, *A*, *B*, and *D*, and the interaction (*AB*) were significant because such effects presented *p* values (*F* test) smaller than 0.05; this indicated that the probability of the null hypothesis was false with 95% confidence. In light of this, the variations observed on the response were due to the input of the studied effects instead of random errors associated with the measures.

Table II presents the ANOVA data obtained for the 2^{4-1} factorial design. The mathematic model, in terms of coded factors, which gives the swelling (S) value as function of significant effects, is represented by eq. (2):

$$S = 228.13 + 63.37A - 91.88B + 32.13D - 23.62AB \quad (2)$$

The model *F* value of 113.84 implied that the model was significant. There was only a 0.14% chance that a model *F* value this large could occur because of noise. Figure 1 shows the predicted

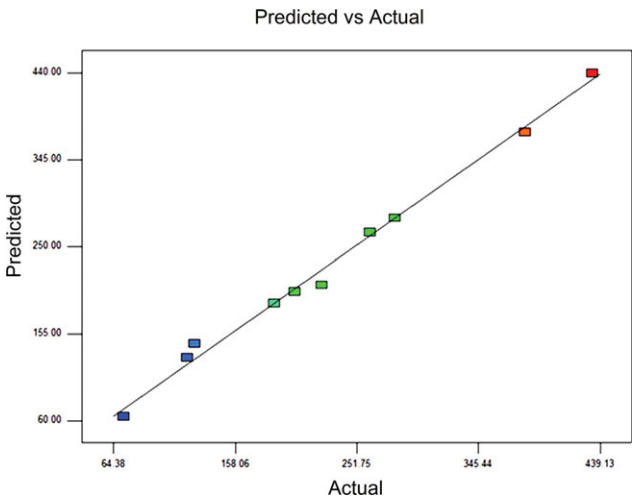

Figure 1. Predicted versus actual response according to FFD. [Color figure can be viewed in the online issue, which is available at wileyonlinelibrary.com.]

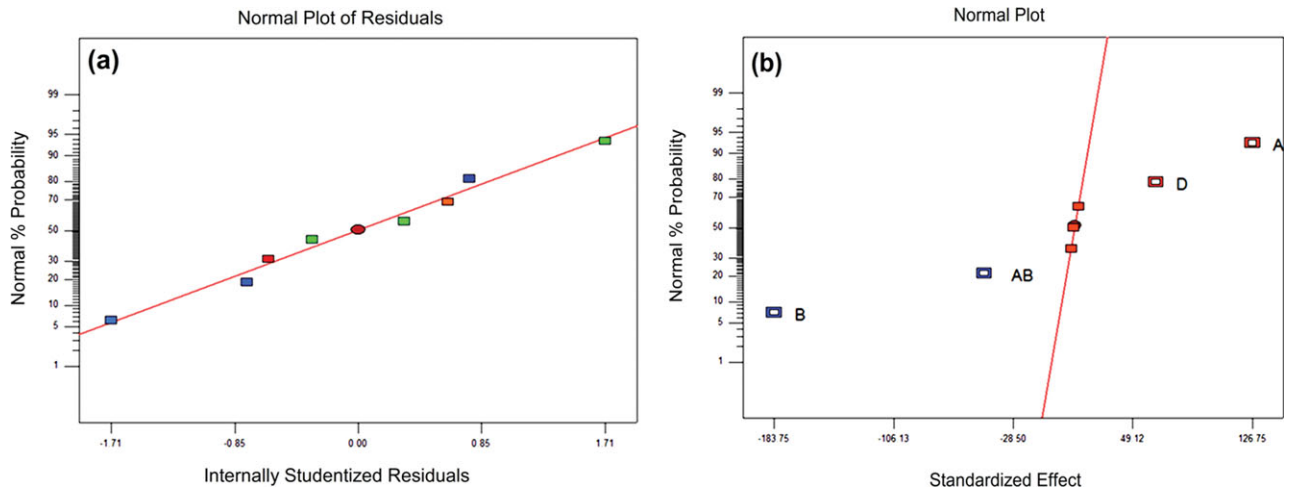

Figure 2. (a) Normal plot of residuals and (b) normal plot. [Color figure can be viewed in the online issue, which is available at wileyonlinelibrary.com.]

versus the actual response. The model fit very well the experimental data.

Considering the normal probability plot, we were able to evaluate whether the data was distributed normally or not from the graphical representation. The residual values explained the differences between the predicted values (model) and the observed ones (experimental). The data was distributted normally when all of the points fell close to the straight line in the normal plot of the residual. In Figure 2(a), it is quite evident that the experimental points were aligned; this suggested a normal distribution, with the data falling in the range of +1.71 to −1.71. As shown in Figure 2(b), the disregarded effects were normally distributted with a mean equal to zero, and the points followed the straight line in the graph, whereas the significant effects did not follow the line.

Table III presents the individual contribution of each factor to the evaluated response. We observed that the most influencing factor was *B* in the hydrogel formation, with almost a 60% contribution, followed by *A*, with about a 30% share.

According to Flory's theory,[28] the crosslinking density is a key factor influencing the capacity of water absorption by the hydrogel network, where the water absorption is inversely proportional to the crosslinking density. Hydrogels formed with a high content of MBA (the crosslinking agent) showed an increase in their crosslinking density due to formation of several crosslinking points among the polymer chains. This reduced the free volume in the hydrogel network and reduced the hydrogel hydrophilicity; this prevented the holding of hydrophilic molecules. In addition, the stretching of the polymer network decreased considerably; this prevented large amounts of liquid from diffusing into the hydrogel matrix.[29] Therefore, the hydrogels formed with high contents of MBA showed lower values of water uptake capcity than the hydrogel formed with low contents.

The influence of *A* on swelling was understood in the following way: when the ratio was increased, there were more AA monomers to be grafted onto the CTS backbone; this increased the hydrophilicity of hydrogel and, consequently, improved the water uptake. Also, the additional Na^+ from the neutralization step provided an osmotic pressure difference between the polymeric matrix and the swelling fluid.[30] Figure 3 presents the surface responses for the different factors.

It is worth mentioning that the following characterization sections were performed using the samples with and without filler that presented the best water uptake, experiments 2 and 6, respectively.

FTIR Spectra

The FTIR spectra of pure CTS, CTS-*graft*-PAA, CTS-*graft*-PAA/NONT, and NONT are shown in Figure 4. The CTS spectrum [Figure 1(a)] exhibited a broad band assigned to —OH stretching and N—H group overlap in the spectral region from 3300 to 3450 cm^{-1}, amide bands at 1658 and 1569 cm^{-1}, and a band at 1020 cm^{-1} assigned to C—O—C stretching. Figure 4(b) shows the FTIR spectrum of CTS-*graft*-PAA, and we observed a characteristic shoulder at 1686 cm^{-1}, which was assigned to C=O vibrational stretching from the —COOH groups proceedings from PAA. In addition, the bands at 1573 and 1410 cm^{-1} were assigned to the asymmetric and symmetric stretching of C=O. The band at 1326 cm^{-1} contributed to the stretching and bending vibrations of the C—N bond of the amide III band. The characteristic absorption bands of N—H and C_3—OH of CTS were displaced and showed different intensities than the same bands observed in the spectrum of pure CTS. The displacement of the N—H band suggested that the grafting of PAA

Table III. Contribution of Each Factor to the Response

Factor	Contribution (%)
A	27.33
B	57.45
D	7.07
AB	3.80

Applied Polymer SCIENCE

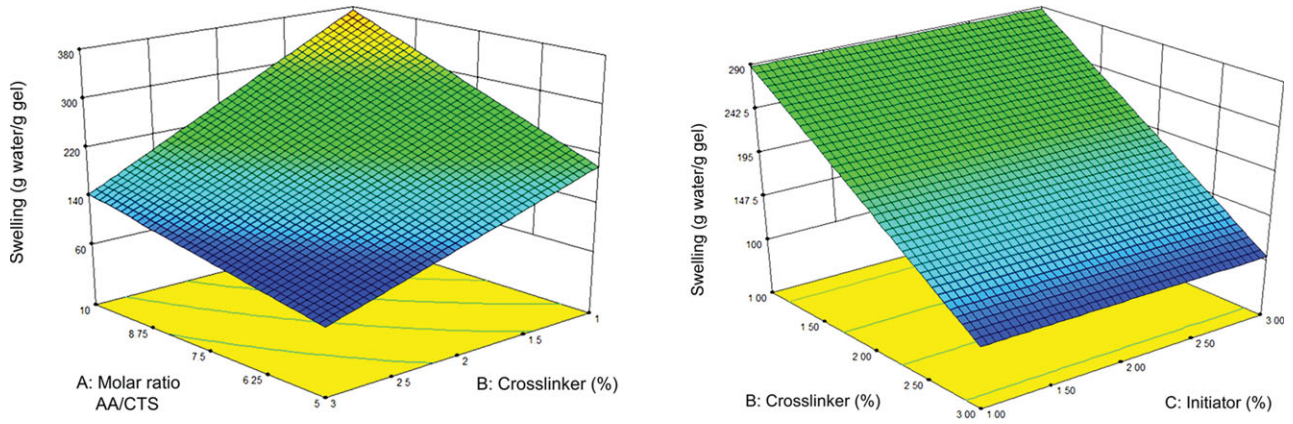

Figure 3. Response surfaces obtained from 2^{4-1} FFD. [Color figure can be viewed in the online issue, which is available at wileyonlinelibrary.com.]

occurred on the amino groups from CTS. Some studies have shown that this behavior suggests the grafting of PAA onto the CTS backbone.[31,32] Furthermore, the appearance of bands at 1457 (C—H), 1410, 1170, and 1070 cm^{-1} indicated the grafting of PAA chains into the CTS backbone.[33,34] The FTIR spectrum of the CTS-*graft*-PAA/NONT hydrogel composite [Figure 4(c)] showed a profile quite similar to the FTIR spectrum of the CTS-*graft*-PAA hydrogel. However, we observed the appearance of characteristics bands of NONT [see Figure 4(d)] at 1035 and 470 cm^{-1}, which represented the Si—O bonds. This suggested that the filler NONT acted as an inert filler inside the hydrogel matrix and that chemical and physical interactions did not occur between the matrix and the filler.

The spectrum of NONT [Figure 4(d)] showed bands at 2840–3000 cm^{-1}, which were related to the stretching of carbon–hydrogen bonds of alkanes, which was due to the presence of organic matter commonly aggregating to such material (a possible contaminant). According to the literature, these bands, proceeding from an organic material, generally appear in the 2929–2858-cm^{-1} range.[31,35]

The large absorption band between 3000 and 3750 cm^{-1} was assigned to the stretching of hydroxyl groups belonging to the octahedral layers and to the water molecules coordinated to cations for ionic compensation.[32,33] The bands assigned to stretching of silicon–oxygen bonds appeared in the region from 960 to 1150 cm^{-1} and were influenced by the composition of atoms on the octahedral layer. The band referent to the silicon–oxygen bond was observed at 1034 cm^{-1}, and the bands in the region from 550 to 960 cm^{-1} were assigned to the octahedral deformations of R—O—H groups (R = Fe^{3+} or Mg^{2+}).[32,33] The strong absorption occurring in the region below 550 cm^{-1} was due to vibrations of ions in the octahedral plane and to its adjacent oxygen atoms.[33]

WAXS

The WAXS pattern of NONT is shown in Figure 5(a) and provided information such as the main mineral constituents and some data of the structural parameters of NONT. The reflections at 7.14° (001) and 19.78° were characteristic of clays whose NONT, a dioctahedral smectite, is re predominant.[36] In the same way, the reflections at 21.7° (101) and 26.6° (011)

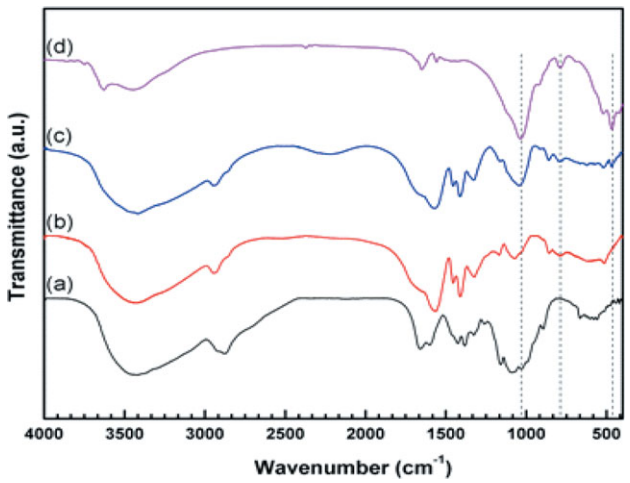

Figure 4. FTIR spectra of the (a) pure CTS, (b) CTS-*graft*-PAA (experiment 6), and (c) CTS-*graft*-PAA/NONT hydrogel composite with 10 wt % NONT (experiment 2), and NONT. [Color figure can be viewed in the online issue, which is available at wileyonlinelibrary.com.]

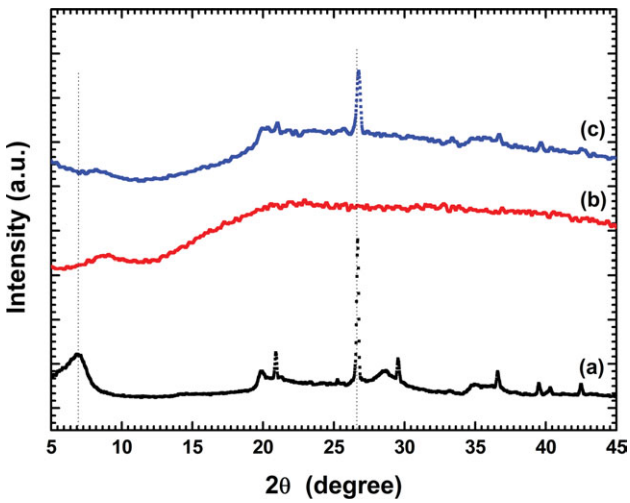

Figure 5. WAXS patterns of the (a) NONT, (b) CTS-*graft*-PAA, and (c) CTS-*graft*-PAA/NONT hydrogel composite. [Color figure can be viewed in the online issue, which is available at wileyonlinelibrary.com.]

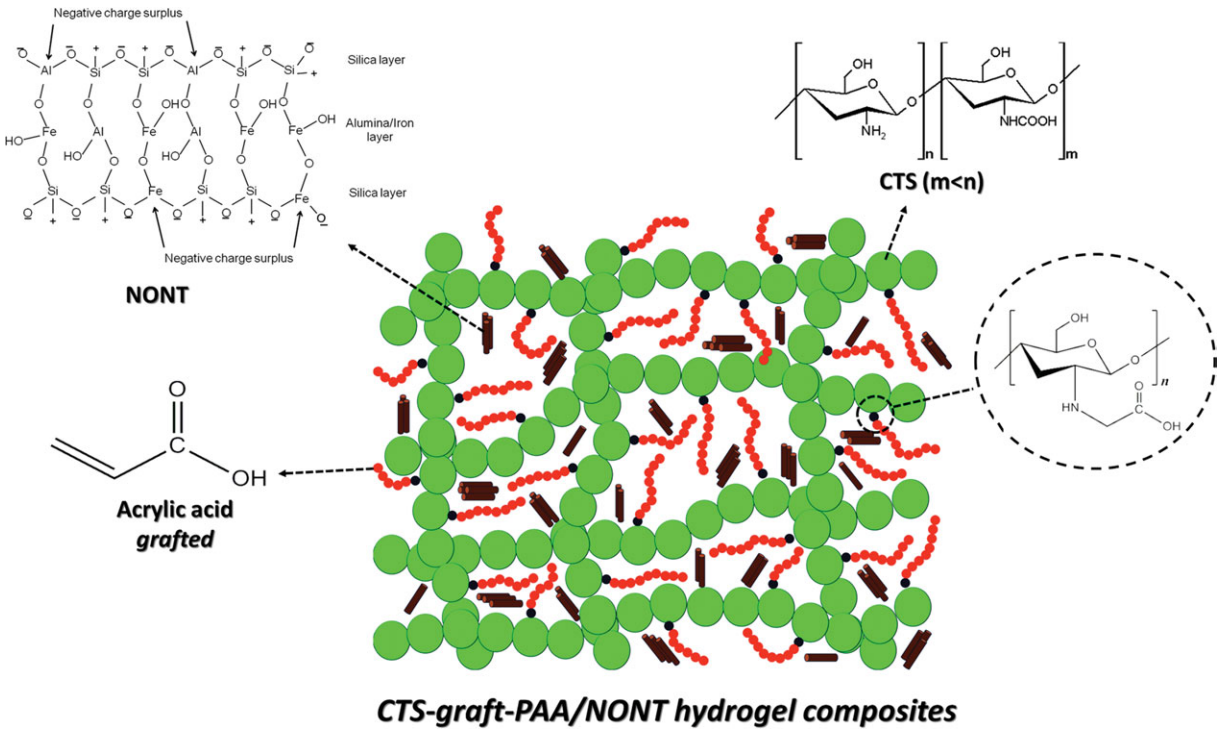

Figure 6. Proposed model for the structure of the CTS-*graft*-PAA/NONT hydrogel composite network. [Color figure can be viewed in the online issue, which is available at wileyonlinelibrary.com.]

characterized the presence of mineral silicon dioxides of cristobalite and quartz, respectively, which are commonly present as impurities in clays, because their particle sizes are very similar to the particle sizes of clay. Thus, they can hardly ever be separated from clay minerals. The WAXS patterns obtained here were in accordance with the works of Mihaboub et al.[37] and Vreysen and Maes.[38]

The WAXS patterns and FTIR data evidenced the formation of the composite hydrogel and suggested the incorporation of NONT into the polymer matrix, as sketched in Figure 6.

SEM

The changes in the morphology of the CTS-*graft*-PAA hydrogel promoted by the addition of NONT were investigated through SEM images (Figure 7). As shown, the CTS-*graft*-PAA hydrogel showed a porous and tight morphology. Despite the fact that they were quite similar, the morphology of CTS-*graft*-PAA/NONT hydrogel composite seemed to be more irregular and quite porous. The main difference found between the two morphologies was related to the pore size. Although the CTS-*graft*-PAA hydrogel had a large pore size with regular distribution, the CTS-*graft*-

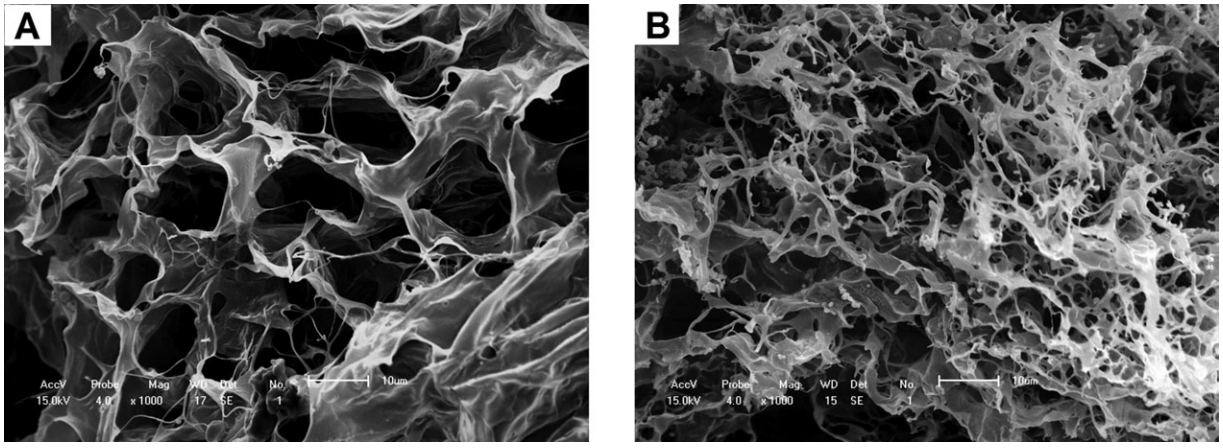

Figure 7. SEM images of the (a) CTS-*graft*-PAA and (b) CTS-*graft*-PAA/NONT hydrogel composite (magnification × 1000, scale 10 μm).

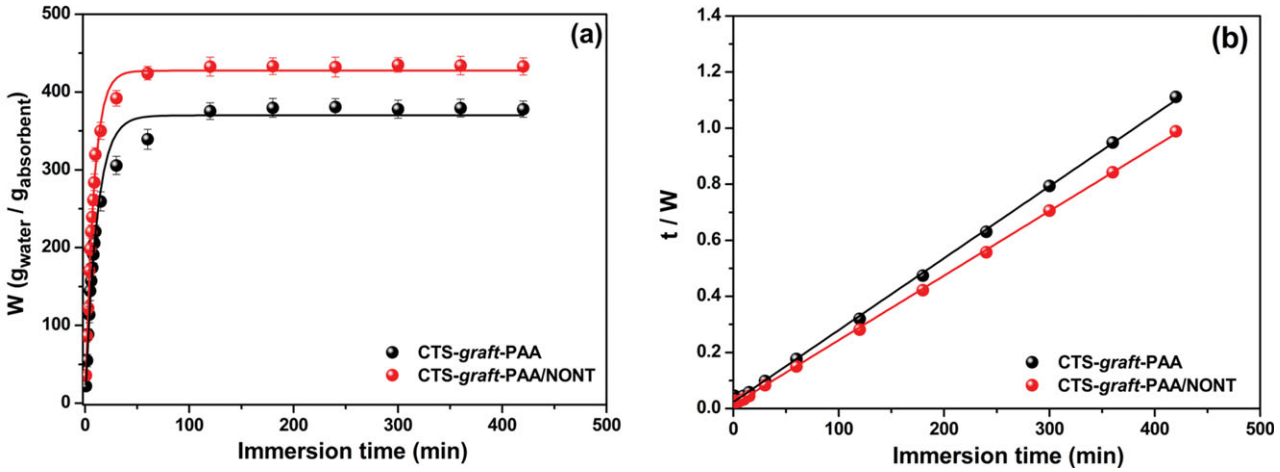

Figure 8. (a) Time-dependent swelling curves and (b) t/W versus t plot for the CTS-*graft*-PAA (experiment 6) and CTS-*graft*-PAA/NONT superabsorbent with 10 wt % NONT (experiment 2) in distilled water. [Color figure can be viewed in the online issue, which is available at wileyonlinelibrary.com.]

PAA/NONT hydrogel had a smaller pore size, and the pores were distributed in an irregular way. Therefore, both kinds of surface allowed a higher influx of water into the polymeric network, which corresponded to superabsorbent composite behavior.

Effect of NONT on the CTS-*graft*-PAA/NONT Swelling Kinetics

Figure 8(a) shows the time-dependent swelling curves of the CTS-*graft*-PAA/NONT and CTS-*graft*-PAA hydrogels. The swelling curves of both hydrogels showed that they had a similar swelling profile. For both the hydrogels, the swelling data showed that they absorbed considerable amounts of water (ca. 90% of the equilibrium value) during the first 30 min after immersion. A slow process followed the initial fast absorption until equilibrium was reached at around 60 min. The CTS-*graft*-PAA hydrogel exhibited a water uptake capacity at equilibrium (W_{eq}) of 381 g of water/g of absorbent, whereas the CTS-*graft*-PAA/NONT hydrogel exhibited a W_{eq} of 433 g of water/g of absorbent. From these data, it was possible to infer that the incorporation of NONT into the hydrogel increased the water uptake capacity. The NONT, cationic clay, was easily ionized; this increased its hydration and distention ability. Once it was dispersed into the hydrogel matrix, the NONT increased its hydrophilicity, and this affected the swelling capacity positively. Similar results were observed by Spagnol et al.,[11] who evaluated the swelling properties of a CTS-*graft*-poly(acid acrylic) matrix with and without cellulose nanowhiskers. The hydrogel filled with cellulose nanowhiskers (a hydrophilic filler) showed a higher swelling capability than the hydrogel without one.

Some of the characteristics collected from the swelling curves through the relations proposed by Karadag et al.[39] are shown as follows:

$$t/W = A + Bt \tag{3}$$

Linear equation of Figure 8 (b) where t is the immersion time.

Where

$$A = \frac{1}{k_s W_t^2} \tag{4}$$

$$B = \frac{1}{W_t} \tag{5}$$

where the A parameter corresponds to the initial swelling rate $[(dW/dt)_0]$ of the hydrogel, k_s is the rate constant for swelling, W_t is the theoretical swelling value at equilibrium, and k_{is} is the initial swelling constant ($k_{is} = k_s W_{eq}^2$). W_t and k_s were calculated by the fitting of the experimental data shown in Figure 8(b) to eqs. (3), (4), and (5). The values for these parameters are presented in Table IV.

In Table IV, it is shown that the equilibrium swelling values were very close to the theoretical equilibrium swelling values; this suggests that eq. (3) fit the experimental data very well. It

Table IV. Parameters Obtained from the Swelling Kinetics

Sample	W_{eq}[a]	W_t[b]	t_{eq} (min)	k_s[d]	k_{is}[e]	R^2
CTS-g-PAA	381 ± 10	389	46 ± 3	2.86×10^{-4}	41.52	0.999
CTS-g-PAA/NONT	433 ± 11	442	34 ± 2	4.01×10^{-4}	75.18	0.999

[a]Equilibrium swelling (g of water/g of absorbent), [b]Theoretical equilibrium swelling (g of water/g of absorbent), [d]Rate of swelling [(g of water/g of absorbent)/min], [e]Initial swelling constant [(g of water/g of absorbent)/min].

Table V. W_{eq} (g of water/g of absorbent) Values of the CTS-*graft*-PAA and CTS-*graft*-PAA/NONT Hydrogel Composites in Aqueous Solutions with Different Salts[a]

	CTS-*graft*-PAA		CTS-*graft*-PAA/NONT	
Salt	W_{eq}	f	W_{eq}	f
NaCl	36.7 ± 0.7	0.90	65.2 ± 1.3	0.85
$CaCl_2$	14.3 ± 0.5	0.96	21.1 ± 0.7	0.95
$AlCl_3$	7.5 ± 0.5	0.98	14.3 ± 0.7	0.97

[a]Concentration = 0.15 mol/L.

was important that the hydrogel composite presented a higher water uptake capability, higher swelling rate, and consequently, a faster equilibrium time (t_{eq}) than the hydrogel without filler, and this effect was attributed to the presence of NONT, which provided high amounts of hydrophilic groups, which improved the performance of the hydrogel.

Effect of the Salt Solution on the Water Absorbency. The characteristics of an external solution, such as the charge valences and salt concentration, greatly influence the swelling behavior of superabsorbent polymers. The swelling of absorbents in saline solutions decreases appreciably compared to that in deionized water. The well-known undesired swelling loss is often attributed to a charge screening effect of the additional cations, which causes a nonperfect anion–anion electrostatic repulsion. Therefore, the osmotic pressure results from the mobile ion concentration difference between the gel and the aqueous phases decreasing; consequently, the absorbency also diminishes.[40] In this study, the influence of some cations on the swelling capability of the hydrogels was tested by the addition of different saline solutions, including monovalent (NaCl), divalent ($CaCl_2$), and trivalent ($AlCl_3$) ion solutions, at 0.15 mol/L and 25.0°C, as the swelling fluids. To achieve a comparative measure of the salt sensitivity of the hydrogels, a dimensionless salt sensitivity factor (f) was defined as follows:[41]

$$f = 1 - \left(\frac{W_{saline}}{W_{water}}\right) \quad (6)$$

where W_{saline} and W_{water} are the swelling capacities in saline solution and deionized water, respectively. The f values (Table V) indicated that the CTS-*graft*-PAA/NONT hydrogels suffered less influence of the presence of salt than the CTS-*graft*-PAA gel. The increase in the ionic strength reduced the difference in the concentration of movable ions between the polymer matrix and the external solution (osmotic swelling pressure) and led to an immediate contraction of the gel.

The decrease was more significant for Ca^{2+} and Al^{3+} ions; this could have been caused by the complex formation ability of carboxamide or carboxylate groups, including intramolecular and intermolecular complex formations, or because one multivalent ion was able to neutralize several charges inside the gel.[42,43] Consequently, the crosslink density of the network increased, whereas the water absorption capacity decreased.

Equilibrium Swelling in Solutions with Various pH Values

The equilibrium swelling behavior of the hydrogels formed in this study was investigated as a function of pH at a fixed ionic strength ($I = 0.1$). Figure 9(a) shows the pH-dependent swelling curves of the CTS-*graft*-PAA and CTS-*graft*-PAA/NONT hydrogels, respectively. According to the data, it was possible to infer that both hydrogels exhibited a clear pH-sensitive swelling capability. The W_{eq} values increased as the pH increased from 2 to 12. Comparing these results with the results previously published by Spagnol et al.,[11] we realized that the incorporation of a filler into a CTS-*graft*-PAA matrix did not affected the swelling capability in media with different pHs. However, in both studies, it was observed that the hydrogel composites showed higher W_{eq} values than simple hydrogels in all of the pH

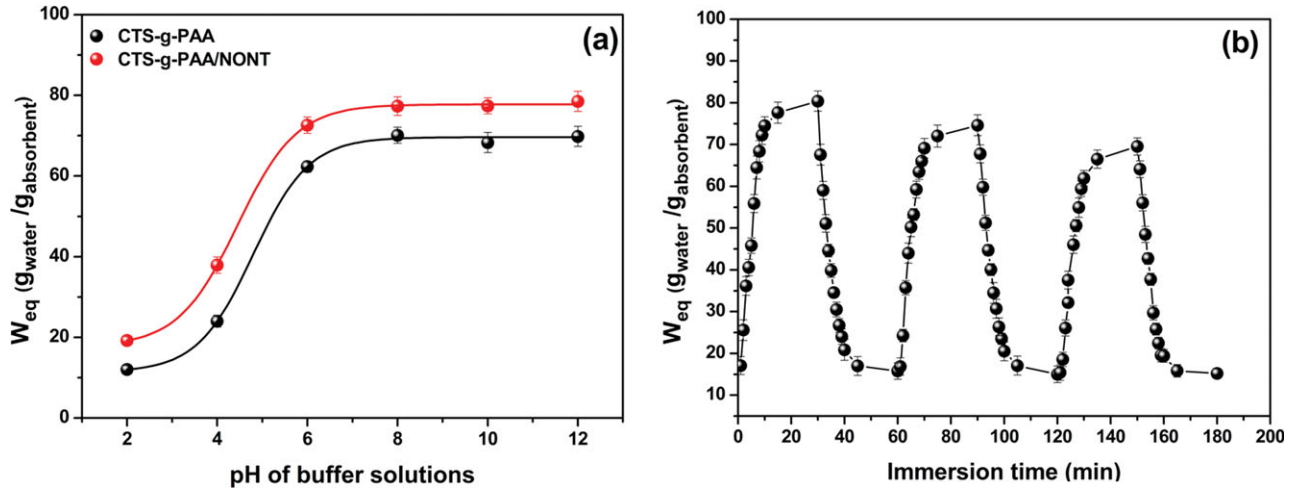

Figure 9. (a) pH-dependent swelling curves for CTS-*graft*-PAA (experiment 6) and CTS-*graft*-PAA/NONT superabsorbent hydrogel with 10 wt % NONT (experiment 2). (b) On–off switching behavior as reversible pulsatile swelling (pH 8.0) and deswelling (pH 2.0) of the CTS-*graft*-PAA/NONT superabsorbent with 10 wt % NONT. The time interval between pH changes was 30 min. [Color figure can be viewed in the online issue, which is available at wileyonlinelibrary.com.]

conditions tested. This variation in the swelling capability was attributed to changes in the protonation of the carboxylic groups from PAA according to pH variations. When the CTS-*graft*-PAA hydrogels were swollen in a pH range of 2–4, the carboxylic groups from PAA ($pK_a \approx 4.57$) were not ionized; this prevented the hydrogel network from suffering from some destabilization due to anion–anion repulsive forces. Therefore, the hydrogel matrix remained entangled enough to prevent a higher liquid content from being absorbed, and this increased the swelling. When the pH of the media was increased to the range of 6–8, the carboxylic groups were in their ionized form; this increased the anion–anion repulsive forces and destabilized the hydrogel matrix. This effect caused the hydrogel matrix to expand, and the amount of liquid absorbed increased considerably, as shown by the increase in the swelling curves.[44,45] On the other hand, at higher pH (pH $>$ 8), the carboxylic groups from PAA remained in their neutral form because of the excess of negatively charged ions in the media. This resulted in a decrease in the repulsion among polymeric chains and, consequentially, in a decrease of the liquid absorbency.

Considering the pH-responsiveness behavior presented by the studied hydrogels and the possibility of such materials to be used as systems for the controlled release of solutes, we feel that an important feature is the ability of those hydrogels to perform many cycles of swelling and deswelling without losing performance. Figure 9(b) shows the reversible swelling–deswelling characteristic of the hydrogels at 25°C through variation of the pH values of the immersion solution from 2.0 to 8.0. As was expected for a hydrogel containing carboxylate groups at pH 8.0, the hydrogel swelled up to about 78 g of water/g of absorbent because of anion–anion repulsive electrostatic forces, whereas at pH 2.0, it decreased within a few minutes because of the protonation of carboxylate groups. Similar on–off switching behavior has been reported.[42,46] It is worth mentioning that both swelling and deswelling happened in a few minutes, and the system presented a minimum loss of performance with three cycles.

CONCLUSIONS

In this article, we have presented new biobased superabsorbent hydrogel composites with great potential for application in several fields because of their pH and salt solution sensitivity. Also, this was the first time NONT clay has been introduced as a filler into the hydrogel matrix to form nanocomposite materials. It was shown that the swelling properties could be tuned through the control of the amount of clay. Furthermore, a complete study of variables influencing the water uptake was performed by the use of FFD. On the basis of the results obtained in this study, one could tune the swelling features of hydrogel composites made of CTS-*graft*-PAA/NONT according to the needs of specific applications.

ACKNOWLEDGMENTS

The authors thank Foundation for the support of Scientific and Technological Development (FUNCAP) (contract grant numbers BPI 0280-106/08 and PIL-139.01.00/09), Brazilian National Counsel of Technological and Scientific Development (CNPq) (contract grant number 507308/2010-7), and Coordination for the Improvement of Higher Education Personnel (CAPES) for financial support and Lindomar R. D. da Silva (Universidade Federal do Ceará) and Cícero P. de Moura (Instituto Federal de Educação, Ciência e Tecnologia do Ceará) for supplying NONT.

REFERENCES

1. Kazanskii, K. S.; Dubrovskii, S. A. *Adv. Polym. Sci.* **1992**, *104*, 97.
2. Sannino, A.; Esposito, A.; De Rosa, A.; Cozzolino, A.; Ambrosio, L.; Nicolais, L. *J. Biomed. Mater. Res. Part A* **2003**, *67*, 1016.
3. Jamshidi, A.; Beigi, F. A. K.; Kabiri, K.; Zohuriaan-Mehr, M. *J. Polym. Test.* **2005**, *24*, 825.
4. Elvira, C.; Mano, J. F.; San Roman, J.; Reis, R. L. *Biomaterials* **2002**, *23*, 1955.
5. Piai, J. F.; Lopes, L. C.; Fajardo, A. R.; Rubira, A. F.; Muniz, E. C. *J. Mol. Liq.* **2010**, *156*, 28.
6. Zohuriaan-Mehr, J.; Motazedi, Z.; Kabiri, K.; Ershad-Langroundi, A.; Allahdadi, I. *J. Appl. Polym. Sci.* **2006**, *102*, 5667.
7. Saboktakin, M. R.; Tabatabaie, R. M.; Maharramov, B.; Ramazanov, M. A. *Carbohydr. Polym.* **2010**, *81*, 726.
8. Bhuniya, S. P.; Rahman, M. D. S.; Satyanand, A. J.; Gharia, M. M.; Dave, A. M. *J. Polym. Sci. Part A: Polym. Chem.* **2003**, *41*, 1650.
9. Sionkowska, A. *Prog. Polym. Sci.* **2011**, *36*, 1254.
10. Lazzeri, L.; Cascone, M. G.; Danti, S.; Serino, L. P.; Moscato, S.; Bernardini, N. *J. Mater. Sci. Mater. Med.* **2006**, *17*, 1211.
11. Spagnol, C.; Rodrigues, F. H. A.; Pereira, A. G. B.; Fajardo, A. R.; Rubira, A. F.; Muniz, E. C. *Carbohydr. Polym.* **2012**, *87*, 2038.
12. Spagnol, C.; Rodrigues, F. H. A.; Neto, A. G. V. C.; Pereira, A. G. B.; Fajardo, A. R.; Radovanovic, E.; Rubira, A. F.; Muniz, E. C. *Eur. Polym. J.* **2012**, *48*, 454.
13. Zhang, X.; Huang, J.; Chang, P. R.; Li, J.; Chen, Y.; Wang, D.; Yu, Y.; Chen, J. *Polym.* **2012**, *51*, 4398.
14. Paulino, A. T.; Guilherme, M. R.; Almeida, E. A. M. S.; Pereira, A. G. B.; Muniz, E. C.; Tambourgi, E. B. *J. Magn. Magn. Mater.* **2009**, *321*, 2636.
15. Cândido, J. S.; Leitão, R. C. F.; Ricardo, N. M. P. S.; Feitosa, J. P. A.; Muniz, E. C.; Rodrigues, F. H. A. *J. Appl. Polym. Sci.* **2011**, *123*, 879.
16. Sirousazar, M.; Kokabi, M.; Hassan, Z. M. *J. Appl. Polym. Sci.* **2012**, *123*, 50.
17. Shi, X.; Wang, W.; Wang, A. *J. Compos. Mater.* **2011**, *45*, 2189.
18. Darvishi, Z.; Kabiri, K.; Zohuriaan-Mehr, M. J.; Morsali, A. *J. Appl. Polym. Sci.* **2011**, *120*, 3453.
19. Hékiniam, R.; Hoffert, M.; Larque, P.; Cheminee, J. L.; Stoffers, P.; Bideau, D. *Econ. Geol.* **1993**, *88*, 2099.
20. Frost, R. L.; Ruan, H.; Kloprogge, J. T.; Gates, W. P. *Thermochim. Acta.* **2000**, *346*, 63.

21. Pillai, C. K. S.; Paul, W.; Sharma, C. P. *Prog. Polym. Sci.* **2009**, *34*, 641.
22. Wang, H.; Li, W.; Luz, Y.; Wang, Z. *J. Appl. Polym. Sci.* **1997**, *65*, 1445.
23. Fajardo, A. R.; Piai, J. F.; Rubira, A. F.; Muniz, E. C. *Carbohydr. Polym.* **2010**, *80*, 934.
24. Zhang, L.; Rakotondradany, F.; Myles, A. J.; Fenniri, H.; Webste, T. *J. Biomaterials* **2009**, *30*, 1309.
25. Pourjavadi, A.; Mahdavinia, G. R. *Turk. J. Chem.* **2006**, *30*, 595.
26. Abd El-Rehim, H. A.; Hegazy, E.-S. A.; Abd El-Mohdy, H. L. *J. Appl. Polym. Sci.* **2004**, *93*, 1360.
27. Zheng, Y.; Liu, Y.; Wang, A. *Chem. Eng. J.* **2011**, *171*, 1201.
28. Flory, P. J. In Principles of Polymer Chemistry; Cornell University, Ithaca, NY, **1953**.
29. Aouada, F. A.; de Moura, M. R.; Fernandes, P. R. G.; Mukai, H.; da Silveira, A. C. F.; Itri, R.; Rubira, A. F.; Muniz, E. C. *Eur. Polym. J.* **2006**, *42*, 2781.
30. Liu, J.; Wang, Q.; Wang, A. *Carbohydr. Polym.* **2007**, *70*, 166.
31. Wang, Q.; Xie, X.; Zhang, X.; Zhang, J.; Wang, A. *Int. J. Biol. Macromol.* **2010**, *46*, 356.
32. Liu, Y.; Zheng, Y.; Wang, A. *J. Environ. Sci.* **2010**, *22*, 486.
33. Zhang, J.; Wang, L.; Wang, A. *Ind. Eng. Chem. Res.* **2007**, *46*, 2497.
34. Zhang, J. P.; Wang, A. Q.; Wang, A. *Carbohydr. Polym.* **2007**, *68*, 367.
35. Tabak, A.; Afsin, B.; Caglar, B.; Koksal, E. *J. Colloid Interface Sci.* **2007**, *313*, 5.
36. Grim, R. E. In Clay Mineralogy, 2nd ed.; McGraw-Hill: New York, **1968**. p 41.
37. Mahboub, R.; El Mouzdahir, Y.; Elmchaouri, A.; Carvalho, A.; Pinto, M.; Pires, J. *Colloids Surf. A* **2006**, *280*, 81.
38. Vreysen, S.; Maes, A. *Appl. Clay Sci.* **2006**, *32*, 283.
39. Karadag, E.; Uzum, O. B.; Saraydin, D. *Mater. Des.* **2005**, *26*, 265.
40. Liu, H. Q.; Zhen, M.; Wu, R. H. *Macromol. Chem. Phys.* **2007**, *208*, 874.
41. Pourjavadi, A.; Sadeghi, M.; Hoseinzadeh, H. *Polym. Adv. Technol.* **2004**, *15*, 645.
42. Mahdavinia, G. R.; Zohuriaan-Mehr, M. J.; Pourjavadi, A. *Polym. Adv. Technol.* **2004**, *15*, 173.
43. Wang, A.; Zheng, Y.; Zhang, J. E. *Eur. Polym. J.* **2007**, *43*, 1691.
44. Omidian, H.; Rocca, J. G.; Park, K. *J. Controlled Release* **2005**, *102*, 3.
45. Hamshary, H. E. *Eur. Polym. J.* **2007**, *43*, 4830.
46. Richter, A.; Bund, A.; Keller, M.; Arndt, K. *Sens. Actuators B* **2004**, *99*, 579.